Tor Vergata Synoptic Solar Telescope

Spectral Characterization of Potassium KI D1 MOFs

Daniele Calchetti[a], Giorgio Viavattene[a,b], Luciano Terranegra[c], Ermanno Pietropaolo[d], Maurizio Oliviero[c], Neil Murphy[e], Stuart M. Jefferies[f], Luca Giovannelli[a], Dario Del Moro[a], and Francesco Berrilli[a]

[a]Department of Physics, University of Rome Tor Vergata, Via della Ricerca Scientifica 1, 00133, Rome, Italy
[b]INAF - Astronomical Observatory of Rome, Via Frascati 33, 00078, Monte Porzio Catone, Rome, Italy
[c]INAF - Astronomical Observatory of Capodimonte, Salita Moiariello 16, 80131 Napoli, Italy
[d]INFN-GSGC L'Aquila and DSFC University of L'Aquila, Via Vetoio, 67100 Coppito, L'Aquila, Italy
[e]Jet Propulsion Laboratory - NASA, 4800 Oak Grove Drive, Pasadena, CA 91109, USA
[f]Department of Physics and Astronomy, Georgia State University, 33 Gilmer Street, SE Atlanta, GA 30303, USA

ABSTRACT

Synoptic telescopes are fundamental tools in Solar Physics and Space Weather. Their typical high cadence full-disk observations are pivotal to assess the physical conditions on the Sun and to forecast the evolution in time of those conditions.
The TSST (Tor vergata Synoptic Solar Telescope) is a synoptic telescope composed of two main full-disk instruments: an Hα Daystar SR-127 telescope and a Magneto Optical Filter (MOF)-based telescope in the Potassium KI at 769.90 nm. The MOF consists in a glass cell containing a Potassium vapor where a longitudinal magnetic field is applied and which produces two passing bands on the wings of the solar absorption line of Potassium. This project started in 2011, in collaboration with the research groups involved in MOTH (IfA, GSU and JPL) and VAMOS experiment (INAF-OACN), but it was slowed down due to the reduction of available funds.
The Hα images are used for the real-time detection of flaring regions. The MOF-based channel produces full disk Line-of-Sight magnetic field and velocity maps of the solar photosphere at $\sim$300 km above the solar surface. Magnetograms are essential for the study of the magnetic field's topology in active regions, while the dopplergrams are used to study the dynamics of the solar atmosphere.
In this work, we present the optical setup and spectral characterization of the MOF-based telescope. We also present details on the spectral characterization of the MOFs cells which is a required test to obtain calibrated magnetograms and dopplergrams.

Keywords: Synoptic solar telescope, space weather, MOF, magnetograms, H-alpha

1. INTRODUCTION

The capability to monitor and forecast the environmental conditions in Geospace (space weather) is of paramount importance for our technological society. Sudden changes in space conditions, due to solar wind or eruptive events such flares and coronal mass ejections (CME), can distort communications and GNSS signals; interfere with global surveillance operations; generate geomagnetically induced currents (GIC) entering the power grids; and negatively impact the performance and longevity of human space assets.[1] In order to understand the physical mechanisms underlying the solar events affecting the Space Weather and to create reliable flare and CME

Further author information: (Send correspondence to L.G.)
L.G.: E-mail: luca.giovannelli@roma2.infn.it

Ground-based and Airborne Telescopes VIII, edited by Heather K. Marshall, Jason Spyromilio, Tomonori Usuda, Proc. of SPIE Vol. 11445, 114452T · © 2020 SPIE
CCC code: 0277-786X/20/$21 · doi: 10.1117/12.2562454

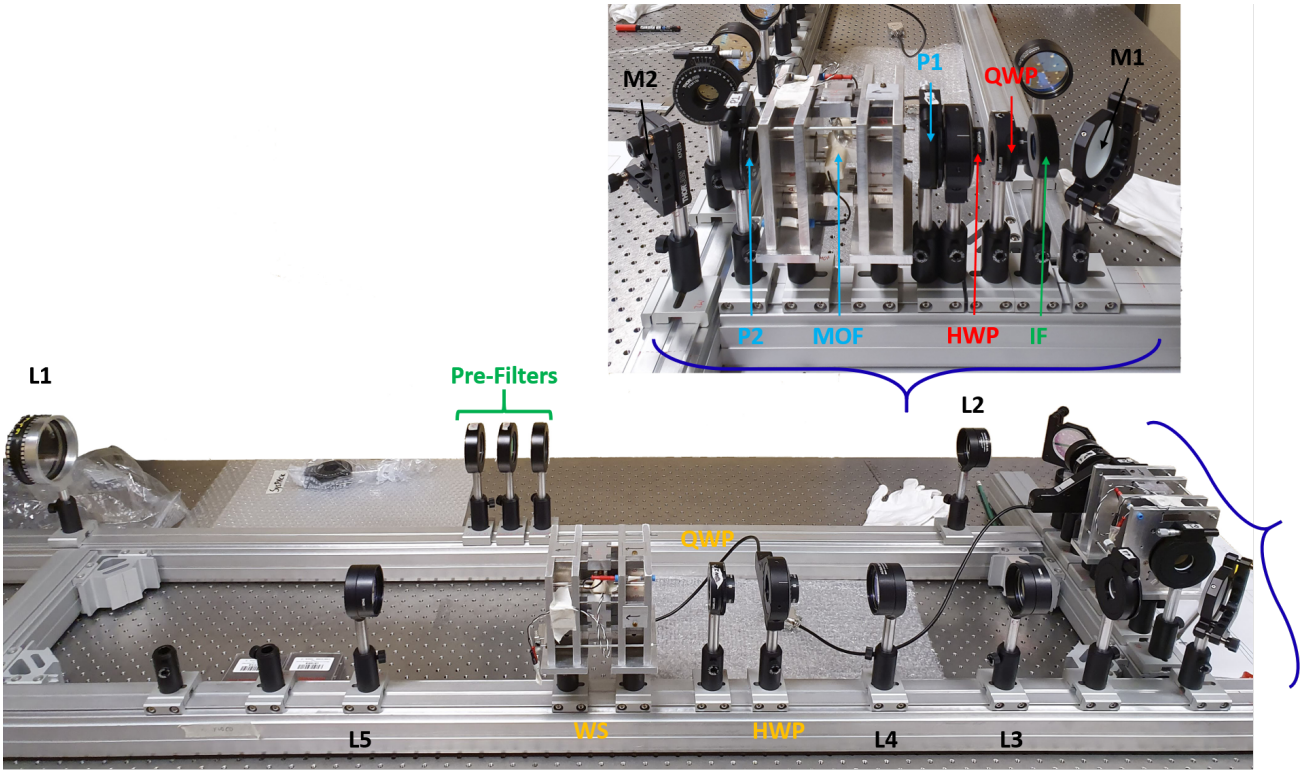

Figure 1. Optical scheme of the MOF-based channel of the TSST. Lenses and mirrors are indicated in black, filters in green, polarization selector in red, MOF section in blue and WS section in orange. Top panel shows the polarization selector and the MOF section between two folding mirrors. The picture was acquired during the assembly phase of the channel.

forecasting algorithms the continuous monitoring of the Sun is essential. In particular, it is necessary to guarantee continuous coverage of the magnetic and dynamic state of our star. This is possible through dedicated space missions (e.g., SOHO, SDO, LAGRANGE) or through networks of solar synoptic telescopes (e.g., GONG) capable of producing magnetic, velocity and intensity maps of the solar photosphere.

Actually, the roots of open structures and magnetic loops that extend into the solar corona have their origin in the photosphere. The photospheric advection flows, associated to the turbulent convection that occurs in the underlying plasma layers, govern the coronal magnetic structures and, ultimately, induce the instabilities underlying the explosive events (i.e., flares and CMEs) connected to sudden changes in the physical status of interplanetary and circumplanetary space. The photospheric magnetic field, and its extensions in the chromosphere and corona, finally determines the presence of the Coronal Holes (CHs), structures connected to the variations of fast and slow solar wind, when an imbalance in the distribution of the signed photospheric magnetic field is created.

In the context of research on Space Weather, and especially in relation to the continuous monitoring of solar activity through multi-band spectro-polarimetric observations, networks of synoptic ground-based telescopes are very important. Especially, if these networks are developed in the direction of having low cost telescopes, to ensure a high degree of diffusion and an appropriate longitude coverage, and if they are designed to be managed in a robotic way. The Tor Vergata Synoptic Solar Telescope (TSST) project is designed in this light. In fact, the TSST is a low-cost, small and robotic multi-band instrument conceived to provide magnetic and velocity maps of the solar atmosphere and to be compliant to the principal goals of modern synoptic projects, e.g., the SPRING project developed under the H2020-SOLARNET program and focused on design studies of synoptic solar facilities.[2]

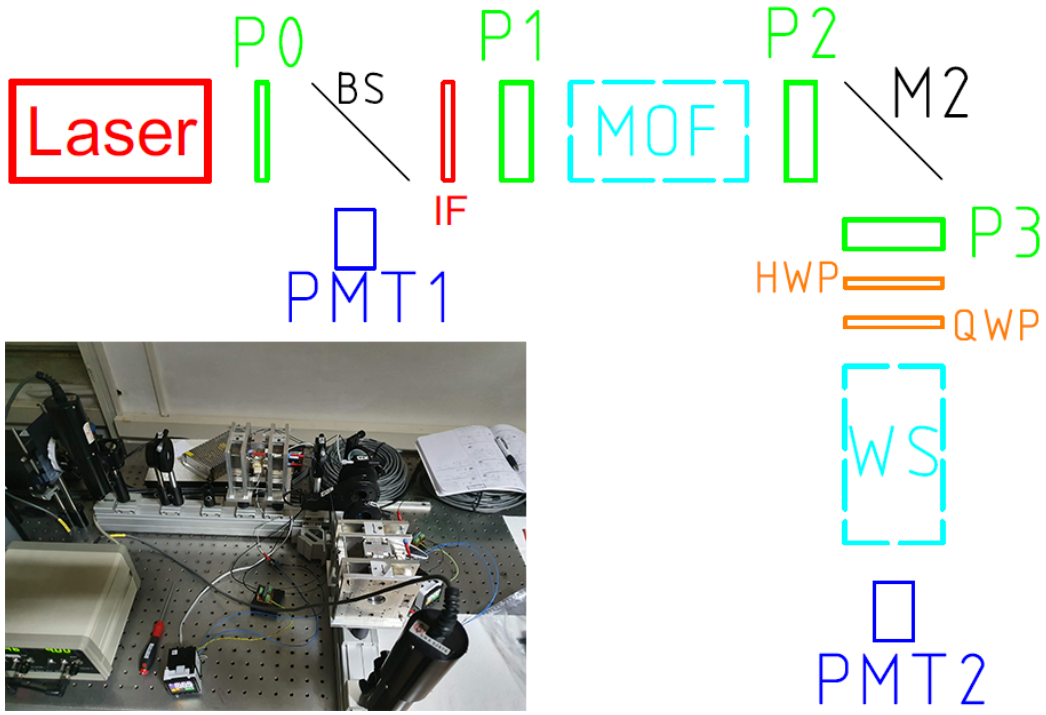

Figure 2. The optical scheme used during the spectral calibration. P0, P1 and P2 are linear polarizers, BS is a beam-splitter, IF is the interference filter, MOF and WS are two potassium cells, M2 is a flat mirror, HWP is a half-wave plate, QWP is a quarter-wave plate, and PMT1 and PMT2 are photomultiplier tubes. *Bottom left*: Picture of the setup during the measurements.

2. THE TOR VERGATA SYNOPTIC SOLAR TELESCOPE (TSST)

The Tor Vergata Synoptic Solar Telescope (TSST) is composed by two channels: a Hα chromospheric channel operating at 656.28 nm and a custom channel based on potassium KI D1 Magneto-Optical Filter (MOF)[3,4] at 769.90 nm.

The Hα telescope is a COTS 127 mm achromatic refractor (f=2667 mm) telescope Daystar SR-127 QT with a narrow band filter (passband = 0.04 nm) centered at the Hα line. The narrow band filter (NBF) is a temperature stabilized etalon in collimated configuration. It is the NBF used in the Hα channel GONG network to monitor the chromospheric transients.[5] The Hα optics contains a focal reducer and field curvature corrector to match the CMOS detector pixel scale of the MOF channel (i.e., 2.6 arcsec/pixel).

The MOF-based channel is based on a custom mechanical and optical design. The optical setup for the potassium KI D1 MOF (Fig. 1) employs a Melles-Griot doublet (focal length 1200mm, aperture 80mm). The optical and polarimetric scheme of this channel is discussed in detail in Ref. 6,7.

Magnetic maps of the solar photosphere are essential to investigate solar activity and for Space Weather studies and services, particularly related to event (e.g., CMEs or flares) forecasting.[8–14] While, velocity maps of the solar surface are fundamental to study the dynamics of the Sun, the turbulent convection[15,16] and the propagation of waves through the solar atmosphere.[17–20] MOF-based telescopes have always been used for helioseismology and to study the propagation of waves through the solar atmosphere as well, particularly using multi-height Dopplergrams.[19,21,22]

In the next section we will focus on the spectral characterization of MOF filters, the optical alignment procedure and the opto-mechanical assembly. These aspects are essential for the proper functioning of telescopes based on MOF filters.

2.1 Spectral Characterization of Potassium KI D1 MOF filters

The procedure to characterize the spectral response of potassium KI D1 MOFs consists of:

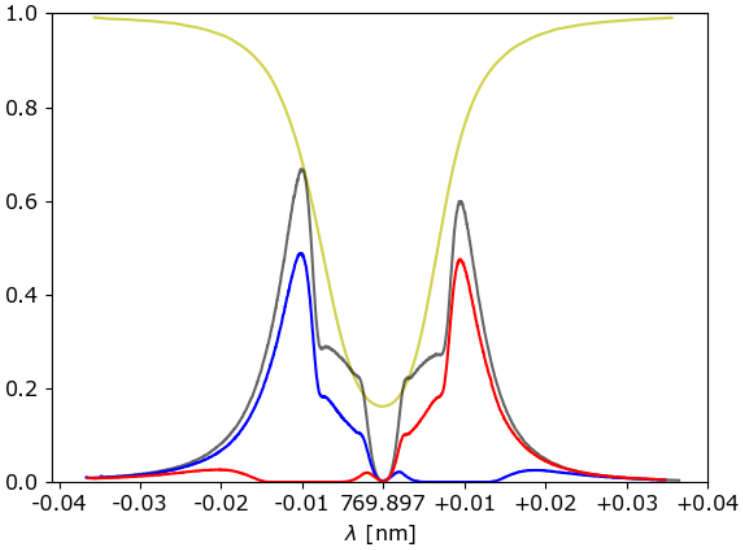

Figure 3. Measured MOF passband (black plot) and red and blue passbands at working temperatures. A representation of the undisturbed potassium absorption KI D1 line (yellow plot) is superimposed as a comparison.

- tuning the MOF's temperature and magnetic field to obtain a distance of ~ 0.02 nm between the blue and red peaks of the passband;
- matching the absorption passband of the WS with the MOF peaks by tuning the magnetic field of the WS;
- finding the angles of the axes of each optical elements to maximize the transmission and minimize the leakages;
- tuning the temperature of the WS to remove one peak of the MOF passband altogether.

The experimental setup, at the INAF Astronomical Observatory of Capodimonte facility, used to carry out the steps previously described is composed by a tunable diode laser having a wavelength tuning step of 3.96×10^{-5} nm at 770 nm and whose beam have a FWHM $< 1 \times 10^{-5}$ nm.[23,24] The system includes a linear polarizer placed in front of the laser and two photomultiplier tubes (PMTs) with tunable gains.
The optical scheme used for this procedure is shown in Fig. 2. P0 is the first linear polarizer, which is not part of the telescope and avoids spurious variation of transmission due to possible changing of laser beam polarization. BS is a beam-splitter used to produce a light beam towards the first PMT. M2 is the only mirror placed in the laser setup which corresponds to M2 of the optical setup of the telescope, described in Ref. 6. Little displacements of M2 are made in the transmission measurements to evaluate and eventually minimize spurious polarization signals generated by the light reflection on the mirror itself. The IF is used to verify its passband and replicate the final optical design of the telescope.[6] P1, P2, and P3 are placed in the same rotating mount with a micrometer fine drive adjuster and a sensitivity of $\sim$2.4 arcmins. Quarter wave plate (QWP) is placed in a rotating mount with a sensitivity of $\sim$5 arcmins. The half wave plate (HWP) mount is motorized, with a rotation speed up to 25°/s and a repeatable incremental motion of 1.8 arcmins. The rotation speed of this mount, and the exposure time of the camera, set the minimum time required to acquire a complete set of four images, which correspond to the blue and red passbands of the TSST in the left and right polarization states of the incoming solar light. These states are selected by a polarization analyzer placed before the MOF section in the TSST setup. It is composed by a QWP and a HWP mounted in a similar way as the corresponding wave plates in Fig. 2. Two PMTs are needed to measure the transmission of all the optical elements with respect to the signal of the laser. For this reason, the passbands of the instrument are expressed as the ratio between PMT2 and PMT1.
The choice of the magnetic field inside the cell has been made in a preliminary spectral characterization presented in Ref. 25. More in detail, the magnetic fields chosen for the Magneto-Optical Filter (MOF) and the Wing Selector

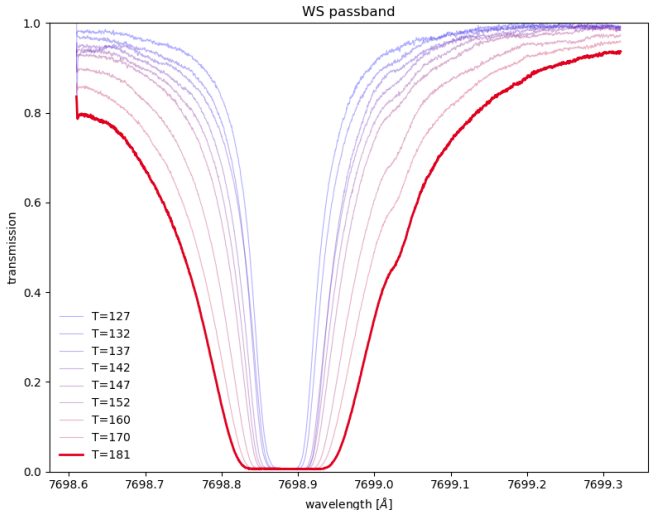

Figure 4. Measured absorption due to the WS section acquired during the preliminary spectral calibration campaign.[25]

(WS) cells are 1.23 kG and 2.26 kG, respectively. We also verified that the gradient of the field is negligible in the center of the holder; this means that the vapor inside the cell is affected by a constant and longitudinal magnetic field.

The second step in the calibration is the rotation of the axes of the polarizers to obtain P0∥P1, P1⊥P2 and P3∥P2. We selected the best angle of the polarizer to minimize the spurious signal from M2 with both cells turned off. We found out that if the light reflected by M2 is linearly polarized with an angle of ∼45° to the horizontal axis, the mirror introduces a ∼10% elliptical polarization. P3 then blocks this signal, but we would lose 10% of the signal, and it could introduce out of band leakage signal. Incident vertically polarized light is the best solution; in fact, we did not detect any spurious signal generated by the mirror.

Once P1 and P2 are crossed, we can turn on the MOF cell and set the temperature in order to find a peak separation of ∼0.02 nm. New electronic temperature controller now has a sensitivity of 0.1°C, which is necessary for the stability of the passband of the instrument. The controller is described in Section Optomechanical Assembly of potassium K I D1 MOF channel. Fig. 3 shows the MOF section passband (black line) at 166.5°C. Passbands at different temperatures are visible in Ref. 7.

Values of the transmission are calibrated using the inverse Zeeman effect. The magnetic field inside the cell is 1.23 kG, so the Zeeman splitting for the $\sigma^{\pm}$ components will be $\Delta\lambda = \pm 4.54 \times 10^{-3}$ nm, considering an effective Landè factor equals to 1.33.[26] The light inside the MOF cell is linearly polarized. It can be considered as the sum of two opposite circular polarization, so only one of that polarization will be absorbed in correspondence of the $\sigma^{\pm}$ lines (as in the WS). This property means that the inverse Zeeman effect creates two absorption lines with transmission equal to 50% and circularly polarized. Passing through P2, the circularly polarized light is half absorbed so that the transmission will be 25% in correspondence of $\Delta\lambda = \pm 4.54 \times 10^{-3}$ nm. That passband is then calibrated dividing by the values in correspondence of the σ lines and multiplying by 0.25.

Next step is the alignment of the HWP and the QWP to the axes of the polarizers. Considering the typical scheme of a MOF-based telescope (see Fig. 1 in Ref. 25), one QWP and one HWP are part of the polarization selector section (before the MOF section). In contrast, one HWP and one QWP are in the Wing Selector (WS) section (after the MOF section, as in Fig. 2). The axes of the HWPs and the QWPs in the polarization analyzer and WS section have the same angles, so we can align every element even if there is not a polarization analyzer in the setup used for the spectral characterization. The QWP has angle of 45° to P1, whereas the HWP oscillates between 0° and 45° to P1. Firstly, we aligned the HWP by placing it between two crossed polarizers (P1 and P2). If the HWP axis is parallel to P1 axis (0° to P1), P2 should block the light. The rotation is then regulated by the motorized mount. Then we use a combination of two crossed polarizers and two parallel HWPs. The first HWP rotates the polarized light by 45° with respect to P1 axis. The second HWP compensates the rotation so that the light is polarized again at 0° in respect to P1. With this setup the light is blocked by the crossed polarizers, but its polarization axis in between the HWPs is at 45° to P1. The QWPs can be aligned inserting

them in between the HWPs and by rotating their axis to be parallel to the polarized light axis. In this way the QWPs do not affect the polarization of the light which is then blocked by P2.
The last step of the calibration is the tuning of the temperature of the WS cell. Firstly we have to reassemble the optical setup described in Fig. 2, turn on the MOF cell at 166.5°C and turn on the WS in order to find the temperature associated with the best passband. Because the absorption acts on the transmission peak too, the working temperature must be a trade-off between the transmission peak and the absorption of the opposite wing. We found as optimal temperature for the WS the value 185°C. The measured blue and red passbands are shown in Fig. 3. In Ref. 7 can be found more details about the temperature dependence of these passbands. Fig. 4 shows an example of the absorption of the WS measured during a preliminary characterization. Looking at the passbands in Fig. 3, we can measure some of its properties, like transmission peaks and width, the maximum velocity and magnetic field measurable by the instrument, the Doppler noise level corresponding to the temperature sensitivity, and the contamination due to the transmission outside the peak. These features are shown in Tab. 1. It is worth noting that the central wavelength of the MOF reference line has no drift because it is due to the atomic transition of the potassium vapour inside the cell. This physical property is the reason for the extreme stability of MOF transmission profiles. Given the dependence of the Macaluso Corbino effect from the temperature, only a minor shift of the blue and red passbands with respect to the central wavelength is present by varying the cell's temperatures. We estimate a shift of about 3 $\times 10^{-4}$ nm/°C from the measured line profiles,[7] in line with Ref. 27, 28, which corresponds to an equivalent Doppler shifts of 11.7 m/s considering the 0.1°C sensitivity of the temperature controller.

Table 1. Properties of the red and blue passbands of the MOF-based channel of the TSST.

	Blue	**Red**
Transmission Peak	48.9%	47.61%
FWHM	5.62 x 10^{-3} nm	5.11 x 10^{-3} nm
Contamination	∼11%	∼13%
Doppler noise level	∼10 m/s	
Velocity Saturation	±4 km/s	
Magnetic Saturation	±2700 G	

2.2 Optomechanical Assembly of potassium KI D1 MOF channel

The two telescopes of the TSST are mounted on a commercial Sky-Watcher EQ8 PRO Synscan equatorial structure. In designing the telescope and purchasing the various optical and electronic parts, we decided to use COTS parts whenever possible to keep the final cost low. Mechanical parts for connecting and supporting custom optical components were made at the mechanical workshop of the Physics Department Physics Department of the University of Rome "Tor Vergata" and we collaborated with the group of the Department of Physical and Chemical Science (DSFC) of the University of L'Aquila, expert in automation and robotization of astronomical instruments.
In particular, the MOF holders were totally redesigned and realized. They have been designed to keep the magnets along the expected magnetic circuit and to keep the vapor cell inside the longitudinal magnetic field. For this reason, we also designed and realized two mechanical parts that block the cell in order to avoid shifts along the optical axis. In fact, even small mechanical displacements can produce misalignments between the optical axis and the longitudinal magnetic field with an effect on the shape of the passing bands of the MOF system.
The MOF and WS holders are caged in an aluminum box with a heat sink and anti-vibration fan. This structure is mandatory to avoid the heating up of the holder, which could change the density profile inside the cell, and of the telescope box again with possible effect on the shape of the passing bands of the MOF system.
MOF cells of the TSST also have a brand new electronic PID controller that can stabilize the cell temperature with 0.1°C sensitivity. The main object of this system is a digital PID temperature controller. This controller

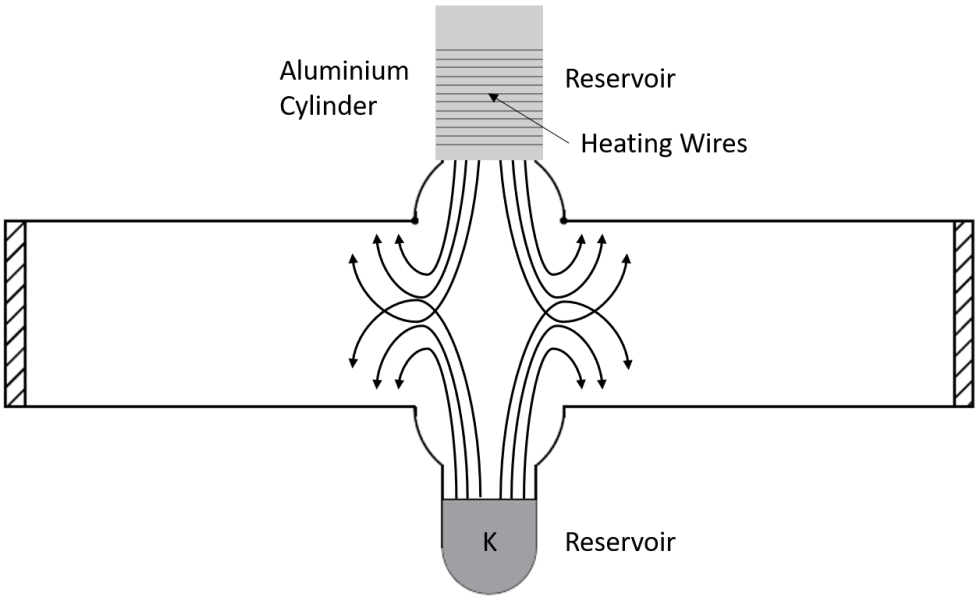

Figure 5. Description of a MOF cell. Optical windows are visible on the left and on the right. The top reservoir is shown with an aluminum cylinder and the heating wires around it. Each reservoir is heated up by 10 Ω resistance (inspired by Ref. 27)

reads the cell's temperature via a pt100 sensor and stabilizes the temperature using an external solid-state relay and 24 V DC power supply that heat wire resistors around the reservoirs of the cell (see Fig. 5). All these components are placed inside the telescope box, where a section is dedicated exclusively to electronic components. These same sensors, coupled with anti-vibration fans, are used to manage the temperature inside the box which contains all the opto-mechanical components of the potassium KI D1 telescope. Baffles and closed tubes are under optimization to block internal reflections and straylight, particularly behind the objective lens, between L2 and L3 and where the three main sections of the MOF optical setup are placed (see Fig. 1 as a reference).

3. CONCLUSIONS

This work presented the complete spectral characterization of the potassium MOF-based channel of the TSST. The spectral characterization of this channel, performed at the INAF Astronomical Observatory of Capodimonte, was mandatory to set the correct temperatures of the MOF cells and to tune the angles of the polarizers and retarders. Results from this test provided a spectral stability of 3×10^{-5} nm. The optomechanical elements of the telescope are COTS parts or realized by the mechanical workshop of the University of Rome Tor Vergata. Final developments of the telescope are now underway. The automatization of the telescope (which consists of camera acquisition and pointing and rotation of the optical elements) is almost completed in collaboration with the University of l'Aquila. The design of the thermal box is almost completed, we are going to mount the two channels of the TSST on their equatorial mount.

ACKNOWLEDGMENTS

This research is partially supported by the Italian MIUR-PRIN grant 2017APKP7T on *Circumterrestrial Environment: Impact of Sun-Earth Interaction*. DC was funded by the Joint Research PhD Program in "Astronomy, Astrophysics and Space Science" between the universities of Roma Tor Vergata, Roma Sapienza and INAF. SMJ was funded by award 1829258 from the National Science Foundation.

REFERENCES

[1] Buzulukova, N., [*Extreme Events in Geospace: Origins, Predictability, and Consequences*], Elsevier Science (2017).

[2] Gosain, S., Roth, M., Hill, F., Pevtsov, A., Martinez Pillet, V., and Thompson, M. J., "Design of a next generation synoptic solar observing network: solar physics research integrated network group (SPRING)," in [*Ground-based and Airborne Instrumentation for Astronomy VII*], Evans, C. J., Simard, L., and Takami, H., eds., *Society of Photo-Optical Instrumentation Engineers (SPIE) Conference Series* **10702**, 107024H (July 2018).

[3] Cimino, M., Cacciani, A., and Sopranzi, N., "An Instrument to measure Solar Magnetic Fields by an Atomic-Beam Method," *Solar Physics* **3**, 618–622 (Apr. 1968).

[4] Agnelli, G., Cacciani, A., and Fofi, M., "The Magneto-Optical Filter. I: Premilinary Observations in Na D Lines," *Sol. Phys.* **44**, 509–518 (Oct. 1975).

[5] Giersch, O., "GONG Inter-site Hα Flare Comparison," in [*Journal of Physics Conference Series*], *Journal of Physics Conference Series* **440**, 012006 (June 2013).

[6] Viavattene, G., Calchetti, D., Berrilli, F., Del Moro, D., Giovannelli, L., Pietropaolo, E., Oliviero, M., and Terranegra, L., "Optical design of the Tor vergata Synoptic Solar Telescope (TSST)," *Nuovo Cimento C Geophysics Space Physics C* **43**, 120 (July 2020).

[7] Giovannelli, L., Berrilli, F., Calchetti, D., Del Moro, D., Viavattene, G., Pietropaolo, E., Iarlori, M., Rizi, V., Jefferies, S. M., Oliviero, M., Terranegra, L., and Murphy, N., "The Tor Vergata Synoptic Solar Telescope (TSST): A robotic, compact facility for solar full disk imaging," *Journal of Space Weather and Space Climate* **10**, 58 (Oct. 2020).

[8] Falconer, D., Barghouty, A. F., Khazanov, I., and Moore, R., "A tool for empirical forecasting of major flares, coronal mass ejections, and solar particle events from a proxy of active-region free magnetic energy," *Space Weather* **9**, S04003 (Apr. 2011).

[9] Piersanti, M., Alberti, T., Bemporad, A., Berrilli, F., Bruno, R., Capparelli, V., Carbone, V., Cesaroni, C., Consolini, G., Cristaldi, A., Del Corpo, A., Del Moro, D., Di Matteo, S., Ermolli, I., Fineschi, S., Giannattasio, F., Giorgi, F., Giovannelli, L., Guglielmino, S. L., Laurenza, M., Lepreti, F., Marcucci, M. F., Martucci, M., Mergè, M., Pezzopane, M., Pietropaolo, E., Romano, P., Sparvoli, R., Spogli, L., Stangalini, M., Vecchio, A., Vellante, M., Villante, U., Zuccarello, F., Heilig, B., Reda, J., and Lichtenberger, J., "Comprehensive Analysis of the Geoeffective Solar Event of 21 June 2015: Effects on the Magnetosphere, Plasmasphere, and Ionosphere Systems," *Sol. Phys.* **292**, 169 (Nov. 2017).

[10] Berrilli, F., Casolino, M., Del Moro, D., Forte, R., Giovannelli, L., Martucci, M., Mergé, M., Napoletano, G., Narici, L., Pietropaolo, E., Pucacco, G., Rizzo, A., Scardigli, S., and Sparvoli, R., "Space Weather services for flare and CME forecasting supported by a multi instrument database," in [*SOLARNET IV: The Physics of the Sun from the Interior to the Outer Atmosphere*], 118 (Jan. 2017).

[11] Napoletano, G., Forte, R., Moro, D. D., Pietropaolo, E., Giovannelli, L., and Berrilli, F., "A probabilistic approach to the drag-based model," *Journal of Space Weather and Space Climate* **8**, A11 (Feb. 2018).

[12] Kilpua, E. K. J., Lugaz, N., Mays, M. L., and Temmer, M., "Forecasting the Structure and Orientation of Earthbound Coronal Mass Ejections," *Space Weather* **17**, 498–526 (Apr. 2019).

[13] Berrilli, F., Casolino, M., Cristaldi, A., Del Moro, D., Forte, R., Giovannelli, L., Martucci, M., Mergé, M., Napoletano, G., Narici, L., Pietropaolo, E., Pucacco, G., Rizzo, A., Scardigli, S., and Sparvoli, R., "Introducing SWERTO: A regional space weather service," *Nuovo Cimento C Geophysics Space Physics C* **42**, 47 (Jan. 2019).

[14] Bigazzi, A., Cauli, C., and Berrilli, F., "Lower-thermosphere response to solar activity: an empirical-mode-decomposition analysis of GOCE 2009-2012 data," *Annales Geophysicae* **38**, 789–800 (June 2020).

[15] Caroli, A., Giannattasio, F., Fanfoni, M., Del Moro, D., Consolini, G., and Berrilli, F., "Turbulent convective flows in the solar photospheric plasma," *Journal of Plasma Physics* **81**, 495810514 (Oct. 2015).

[16] Viavattene, G., Consolini, G., Giovannelli, L., Berrilli, F., Del Moro, D., Giannattasio, F., Penza, V., and Calchetti, D., "Testing the Steady-State Fluctuation Relation in the Solar Photospheric Convection," *Entropy* **22**, 716 (June 2020).

[17] Basu, S., "Global seismology of the sun," *Living Reviews in Solar Physics* **13**, 2 (Aug 2016).

[18] Khomenko, E. and Collados, M., "Oscillations and waves in sunspots," *Living Reviews in Solar Physics* **12**, 6 (Nov 2015).

[19] Jefferies, S. M., Fleck, B., Murphy, N., and Berrilli, F., "Observed Local Dispersion Relations for Magnetoacoustic-gravity Waves in the Sun's Atmosphere: Mapping the Acoustic Cutoff Frequency," *ApJ* **884**, L8 (Oct. 2019).

[20] Abbasvand, V., Sobotka, M., Heinzel, P., Švanda, M., Jurčák, J., del Moro, D., and Berrilli, F., "Chromospheric Heating by Acoustic Waves Compared to Radiative Cooling. II. Revised Grid of Models," *ApJ* **890**, 22 (Feb. 2020).

[21] Finsterle, W., Jefferies, S. M., Cacciani, A., Rapex, P., and McIntosh, S. W., "Helioseismic Mapping of the Magnetic Canopy in the Solar Chromosphere," *ApJ* **613**, L185–L188 (Oct. 2004).

[22] Calchetti, D., Jefferies, S. M., Fleck, B., Berrilli, F., and Shcherbik, D. V., "A New Method for Detecting Solar Atmospheric Gravity Waves," *Phil. Trans. R. Soc. A* **379**, 20200178 (2021).

[23] Oliviero, M., Severino, G., and Esposito, G., "Planning magneto-optical filters for the study of magnetic oscillations of the Sun," *Ap&SS* **328**, 325–329 (July 2010).

[24] Oliviero, M., Severino, G., Berrilli, F., Moretti, P. F., and Jefferies, S. M., "The intensity effect in magneto-optical filters," in [*Solar Physics and Space Weather Instrumentation IV*], Fineschi, S. and Fennelly, J., eds., *Society of Photo-Optical Instrumentation Engineers (SPIE) Conference Series* **8148**, 81480V (Oct. 2011).

[25] Calchetti, D., Viavattene, G., Berrilli, F., Del Moro, D., Giovannelli, L., and Oliviero, M., "Tor vergata Synoptic Solar Telescope: preliminary optical design and spectral characterization," in [*Journal of Physics Conference Series*], *Journal of Physics Conference Series* **1548**, 012005 (May 2020).

[26] Quintero Noda, C., Uitenbroek, H., Katsukawa, Y., Shimizu, T., Oba, T., Carlsson, M., Orozco Suárez, D., Ruiz Cobo, B., Kubo, M., Anan, T., Ichimoto, K., and Suematsu, Y., "Solar polarimetry through the K I lines at 770 nm," *MNRAS* **470**, 1453–1461 (Sept. 2017).

[27] Cacciani, A., Rosati, P., Ricci, D., Egidi, A., Apporchaux, T., Marquedant, R. J., and Smith, E. J., "Theoretical and experimental study of the magneto optical filter," JPL Internal Report #D11900, JPL (1994).

[28] Severino, G., Oliviero, M., and Landi Degl'Innocenti, E., "Simulation of Magneto-Optical Filter Transmission Profiles," in [*The Physics of Chromospheric Plasmas*], Heinzel, P., Dorotovič, I., and Rutten, R. J., eds., *Astronomical Society of the Pacific Conference Series* **368**, 617 (May 2007).